

# Cholesterol Binding to the Alkyl Chains of an Intercalated Surfactant Bilayer

N. V. Venkatasubramanian and S. Vasudevan\*

Department of Inorganic and Physical Chemistry, Indian Institute of Science, Bangalore-560012, India

Received: March 16, 2003; In Final Form: June 26, 2003

Alkyl-chain bilayers can be formed within the galleries of layered inorganic solids by intercalation of long-chain amphiphilic surfactant molecules. It is shown here that cholesterol, normally found in lipid bilayers of biomembranes, can bind to the intercalated bilayer, thereby providing a novel route for the insertion of cholesterol in inorganic solids. The new hybrid material is held together by purely noncovalent, nonionic dispersive forces and is a novel example of supramolecular architecture in the solid state. Additionally, it provides a simple system to understand the nature of cholesterol–hydrocarbon interactions at a molecular level. The rigid sterol ring of the cholesterol is located within the intercalated bilayer and is oriented parallel to the alkyl chains. Its presence affects the conformation of neighboring alkyl chains. An analysis of the methylene progression bands in the infrared spectrum of the intercalated bilayer, with and without cholesterol, indicates that these chains are forced to adopt a rigid, all-trans, planar conformation. Conformational freedom of alkyl chains once-removed appear unaffected.

## Introduction

Long-chain amphiphilic surfactant molecules can be introduced within the interlamellar region of layered inorganic solids to form alkyl-chain bilayers within the galleries.<sup>1–3</sup> The intercalated bilayer bears a striking resemblance to lipid bilayers, which are an integral feature of biomembranes. Here, we exploit this similarity to show that molecules such as cholesterol that bind to the lipid bilayer of cell membranes can also bind to the surfactant bilayers grafted to the inorganic layers of the lamellar solid. Our approach has resulted in successful inclusion of cholesterol in an inorganic solid. The new hybrid material is held together by purely noncovalent, nonionic dispersive forces because the surfactant chosen to form the bilayer is devoid of any functional group. Additionally, we show that cholesterol bound to the confined surfactant bilayer provides a simple system to understand the nature of cholesterol–hydrocarbon interactions and the influence of cholesterol on alkyl-chain conformation.

Cholesterol is a major constituent of the plasma membrane of cells of higher organisms where it has both a structural and functional role.<sup>4</sup> Despite numerous investigations involving simple model two-component bilayer membranes, derived from cholesterol and phospholipids, the nature of interaction between the components and the structural role played by the sterol remain unresolved.<sup>5</sup> What has emerged from a number of experimental efforts is a complex picture of the way in which cholesterol affects the physical properties of the lipid bilayers. It is generally accepted that cholesterol has a condensing effect at temperatures above the gel to liquid crystalline melting transition, decreasing the mobility of lipid chains, and a disordering effect with increased mobility below this transition.<sup>6–10</sup> Spectroscopic studies on a number of model cholesterol–lipid systems have, in general, failed to find any evidence for a cholesterol–lipid complex.<sup>11</sup> Although hydrogen-bonding interactions involving the hydroxyl group of the cholesterol

molecule are present, its structural significance has been discounted because cholesterol binds to lipids having no functional group<sup>12</sup> and even when the hydroxyl group of the cholesterol is removed by oxidation.<sup>13</sup>

The layered host lattice chosen for the present study is cadmium thiophosphate, CdPS<sub>3</sub>.<sup>14</sup> Its host–guest chemistry is representative of many layered inorganic solids, for example, the mica-type silicate clays. It, however, offers the advantage that single crystals can be easily formed, the integrity of which is preserved even after intercalation allowing for orientation-dependent spectroscopic studies. Cadmium thiophosphate consists of sheets of CdPS<sub>3</sub>, built from edge-sharing CdS<sub>6</sub> and P<sub>2</sub>S<sub>6</sub> polyhedra, separated by a van der Waals gap.<sup>15</sup> It undergoes an interesting ion-exchange intercalation reaction in which cationic species are introduced into the van der Waals gap with an equivalent loss of cadmium ions from the layers.<sup>16–18</sup> Intercalation is accompanied by dilation of the lattice, the extent of which depends on the guest species.

We have previously shown that long-chain cationic surfactants, cetyl trimethylammonium (CTA, CH<sub>3</sub>(CH<sub>2</sub>)<sub>15</sub>N<sup>+</sup>(CH<sub>3</sub>)<sub>3</sub>) and octadecyl trimethylammonium (ODTA, CH<sub>3</sub>(CH<sub>2</sub>)<sub>17</sub>N<sup>+</sup>(CH<sub>3</sub>)<sub>3</sub>), may be introduced in the galleries of CdPS<sub>3</sub> by ion-exchange intercalation to form Cd<sub>0.83</sub>PS<sub>3</sub>(CTA)<sub>0.34</sub> and Cd<sub>0.83</sub>PS<sub>3</sub>(ODTA)<sub>0.34</sub>, respectively.<sup>3,19</sup> The intercalated surfactants form a bilayer with the cationic headgroup anchored at the negatively charged, cadmium-deficient Cd<sub>0.83</sub>PS<sub>3</sub> layer with a mean head-to-head distance of 9 Å. Spectroscopic studies have shown that a majority of the methylene units of the bilayer adopt the trans configuration and that the methylene chains are tilted at an angle of 55° away from the interlayer normal.<sup>3</sup> Intercalation of the surfactant functionalizes the internal surface of the galleries of CdPS<sub>3</sub> converting it from a hydrophilic to a hydrophobic surface.<sup>20</sup> Here we show that cholesterol can be solubilized in the hydrophobic interior of the alkyl-chain bilayer formed within the galleries of the layered inorganic solid.

Cholesterol bound to the intercalated surfactant bilayer forms a relatively simple system to investigate the nature of cholesterol–hydrocarbon chain interactions. Because no functional group

\* To whom correspondence should be addressed. E-mail: svipc@ipc.iisc.ernet.in.

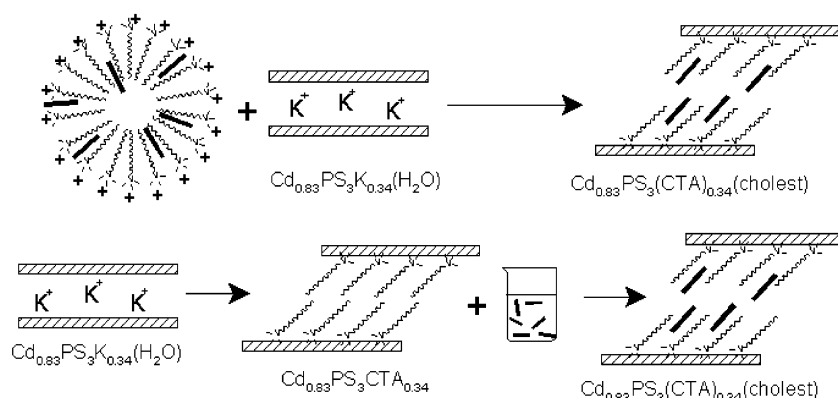
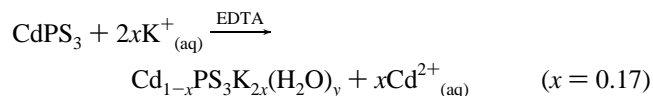


**Figure 1.** Two routes to introduce cholesterol (shown as solid bar) into the galleries of the layered inorganic solid, CdPS<sub>3</sub>.

is present on the intercalated CTA or ODTA ion, hydrogen bonding may be ruled out; interactions between cholesterol and the alkyl chains are, therefore, purely dispersive in character. An additional simplifying factor of these systems, in contrast to actual membrane or other model phospholipid systems, is the absence of cooperative interactions between the methylene tails of the intercalated surfactant ions, and consequently, no phase transitions are exhibited by this system. Cholesterol bound to the intercalated bilayer is therefore an ideal system to investigate changes in alkyl-chain conformation in the presence of cholesterol. In this system, these changes cannot arise from modifications/moderation of chain–chain cooperative interactions but would be a direct consequence of the interaction of cholesterol with the methylene “tail” of the intercalated surfactant.

## Experimental Section

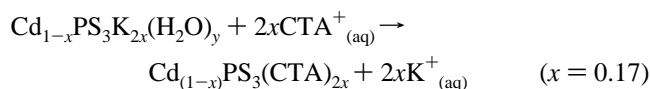
**Materials and Methods.** Cadmium thiophosphate, CdPS<sub>3</sub>, was prepared from the elements; cadmium metal powder, phosphorus, and sulfur in stoichiometric amounts were sealed in quartz ampules at 10<sup>−6</sup> Torr and heated at 650 °C for 2 weeks. CdPS<sub>3</sub> was treated with a 4 M aqueous solution of potassium chloride in the presence of 0.1 M EDTA and 1 M K<sub>2</sub>CO<sub>3</sub>/KHCO<sub>3</sub> as buffer, to give Cd<sub>0.83</sub>PS<sub>3</sub>K<sub>0.34</sub>(H<sub>2</sub>O), in which



hydrated K<sup>+</sup> ions reside in the interlamellar region. The compound has a lattice spacing of 9.4 Å, corresponding to a lattice expansion of 2.8 Å as compared to pristine host CdPS<sub>3</sub>.<sup>18</sup>

Solubilization of cholesterol in the intercalated surfactant bilayer was achieved by the two methods illustrated in Figure 1. In the first method, cholesterol was first solubilized in a water/acetone solution of the surfactant. On addition of Cd<sub>0.83</sub>PS<sub>3</sub>K<sub>0.34</sub>(H<sub>2</sub>O), the hydrated K<sup>+</sup> ions in the galleries ion-exchange with the CTA ions. The cationic surfactant carries the cholesterol molecule with it during the ion-exchange process leading to the introduction of cholesterol within the intercalated bilayer (Figure 1a). In a typical experiment, ~40 mg of cholesterol was dissolved in 0.5 mL of acetone and added to 0.5 mL of 0.1 M aqueous solution of the surfactant with vigorous stirring. The solution was stirred for 4–5 h to accomplish complete dissolution resulting in a turbid solution to which crystals of Cd<sub>0.83</sub>PS<sub>3</sub>K<sub>0.34</sub>(H<sub>2</sub>O) were added. The reaction mixture was not stirred to avoid disintegration of the crystals. A blank experiment was also performed with no added cholesterol. The second method

is a two-step process (Figure 1b) in which the interlamellar potassium ions in Cd<sub>0.83</sub>PS<sub>3</sub>K<sub>0.34</sub>(H<sub>2</sub>O) were first ion-exchanged with CTA ions leading to the formation of the intercalated surfactant bilayer, Cd<sub>0.83</sub>PS<sub>3</sub>(CTA)<sub>0.34</sub>, with a lattice spacing of 33.0 Å. Cadmium ion stoichiometry was established by atomic



absorption spectroscopy (Perkin-Elmer 4381), and that of the intercalated CTA ion was established by CHN analysis (Cd, 29.5%; C, 23.95%; N, 1.53%; H, 4.51%). This compound was then treated with a (0.05 M) hexane solution of cholesterol resulting in a cholesterol–surfactant bilayer. Similar methods were employed for solubilizing cholesterol in the intercalated octadecyl trimethylammonium (ODTA) bilayer. In this case, the lattice spacing of the intercalated bilayer phase, Cd<sub>0.83</sub>PS<sub>3</sub>-(ODTA)<sub>0.34</sub>, is 36.5 Å.

Powder X-ray diffraction patterns were recorded on a Shimadzu-XD-D1 diffractometer using Cu Kα radiation. FT-Raman spectra were recorded on Bruker IFS FT-Raman spectrometer using a Nd:YAG (wavelength 1.064 μm) laser as exciting radiation. All spectra were recorded at 4 cm<sup>−1</sup> resolution with an unpolarized beam. Laser power was kept at 100 mW, and typically ~400 spectra were coadded to improve the signal-to-noise ratio. Infrared spectra were recorded at 4 cm<sup>−1</sup> resolution in the spectral range 400–4000 cm<sup>−1</sup> on a Bruker IFS55 spectrometer. Samples were mounted on a hollow copper block and cooled using a CTI–Cryogenics closed cycle cryostat. Sample temperature could be varied from 300 to 50 K. Infrared spectra for different orientations of the electric field vector (**E**) of the incident IR beam and the interlamellar normal (**C\***) were recorded by an arrangement described in refs 24 and 25. In this arrangement, the crystals are held in the sample block of the cryostat in such a way that the **C\*** axis of the platelet-like crystal is at an angle of 45° with respect the propagation vector of the incident IR beam. From a measurement of the IR spectrum for two different angles of polarization of the electric field vector, **E**, the spectra for **E** ⊥ **C\*** and **E** ∥ **C\*** could be recovered, and subsequently, the spectrum for any orientation,  $\phi$ , of **E** with respect to **C\*** could be calculated.

## Results and Discussion

**Synthesis and Estimation.** Two different methods were used to effect the solubilization of cholesterol in the hydrophobic interior of the intercalated bilayer (Figure 1). In the first, cholesterol is solubilized in aqueous media using a cationic

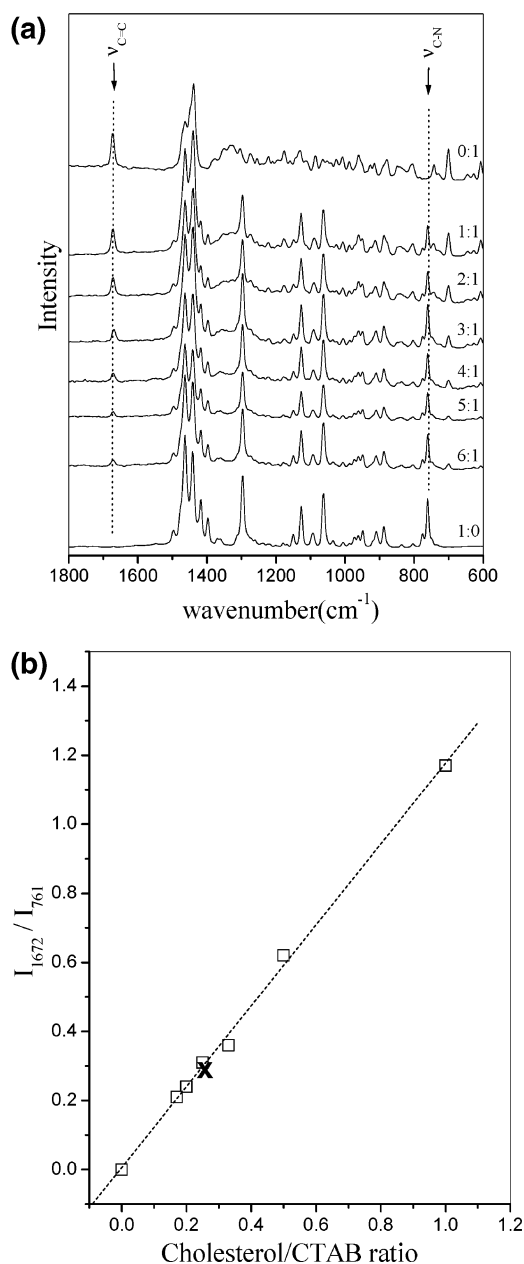


**Figure 2.** The Raman spectra (a) of cholesterol-CTAB physical mixtures for different cholesterol/CTAB molar ratios and the variation in the intensity ratio  $I_{1672}/I_{761}$  (b) for different cholesterol/CTAB molar ratios. The cross (x) indicates the  $I_{1672}/I_{761}$  ratio for the cholesterol-solubilized intercalated bilayer,  $\text{Cd}_{0.83}\text{PS}_3(\text{CTA})_{0.34}(\text{cholesterol})_x$ .

surfactant, either CTA or ODTA. The cationic surfactant with the solubilized cholesterol is then ion-exchanged for preintercalated  $\text{K}^+$  ions in  $\text{Cd}_{0.83}\text{PS}_3\text{K}_{0.34}(\text{H}_2\text{O})$ . The surfactant chains carry the cholesterol molecules with them into the galleries of the inorganic host during the ion-exchange process. The ion exchange is stoichiometric. In the second method, the surfactant cations are first introduced in the host,  $\text{CdPS}_3$ , by ion-exchanging with  $\text{K}^+$  ions in  $\text{Cd}_{0.83}\text{PS}_3\text{K}_{0.34}(\text{H}_2\text{O})$  to form the intercalated bilayer. The functionalized host is then added to a solution of cholesterol in hexane resulting in the adsorption-solubilization of cholesterol in the bilayer.

The concentration of cholesterol in the intercalated phase was determined from the ratio of the integrated intensity of the  $\text{C}=\text{C}$  stretching band of cholesterol ( $1672\text{ cm}^{-1}$ ) and the  $\text{C}-\text{N}^+$  stretching band of the intercalated CTA ion ( $761\text{ cm}^{-1}$ ) in the near-infrared Raman spectra. These modes were chosen because

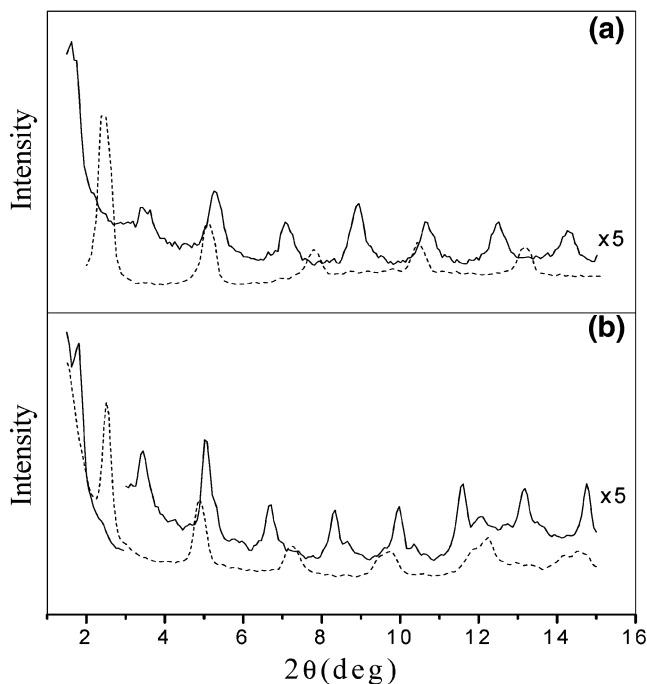


**Figure 3.** X-ray ( $\text{Cu K}\alpha$ ,  $1.54\text{ \AA}$ ) diffraction patterns of the intercalated bilayer with (—) and without (---) solubilized cholesterol for the (a)  $n = 16$  (CTA) and (b)  $n = 18$  (ODTA) bilayer. Solubilization results in an increase in the thickness of the bilayer: for the  $n = 16$  intercalated bilayer, from  $33.0$  to  $49.5\text{ \AA}$ ; for  $n = 18$  bilayer, from  $36.5$  to  $53.5\text{ \AA}$ .

their positions remain unchanged from that in the parent compounds, even after intercalation, and do not suffer from complications arising from overlapping bands (see Supporting Information). A linear relationship of the intensity ratio of these two bands ( $I_{1672}/I_{761}$ ) with that of the concentration ratio of cholesterol/CTAB was established by measuring the Raman spectrum of physical mixtures of cholesterol and CTA bromide at different molar ratios (Figure 2). The cholesterol to intercalated CTA ratio was determined from the  $I_{1672}/I_{761}$  ratio in the Raman spectra of the cholesterol-solubilized intercalated bilayer recorded under identical conditions. The intensity ratio  $I_{1672}/I_{761}$  is  $0.32$ , which corresponds to a solubilized cholesterol to intercalated CTA molar ratio of  $1:4$  or a molecular formula  $\text{Cd}_{0.83}\text{PS}_3(\text{CTA})_{0.34}(\text{cholesterol})_{0.09}$ . It was found that both methods of preparation gave very similar solubilized cholesterol to intercalated CTA (or ODTA) ratios. Attempts to prepare intercalates with cholesterol/CTA ratios different from  $1:4$  by varying initial concentrations were unsuccessful; the products were either biphasic or had unsolubilized cholesterol.

**X-ray Diffraction.** The X-ray diffraction patterns of the cholesterol-bound intercalated surfactant bilayer,  $\text{Cd}_{0.83}\text{PS}_3(\text{C}_n\text{-TA})_{0.34}(\text{cholesterol})_{0.09}$ , along with that of the intercalated surfactant bilayer,  $\text{Cd}_{0.83}\text{PS}_3(\text{C}_n\text{-TA})_{0.34}$ , for the two different chain lengths ( $n = 16$  for CTA and  $n = 18$  for ODTA) are shown in Figure 3. The patterns were recorded for crystals mounted flat on a sapphire disk and hence only  $00l$  reflections are seen in the X-ray diffraction patterns. The series of  $00l$  reflections in the diffraction patterns, in each case, could be indexed to a unique lattice spacing.

Solubilization of cholesterol in the intercalated bilayer is accompanied by dilation along the interlayer axis (Figure 3). It was found that the lattice expansion on solubilization of cholesterol was similar irrespective of the length of the methylene chain of the bilayer. For the intercalated CTA ( $n = 16$ ) ion, the interlayer spacing increases from  $33.0$  to  $49.5\text{ \AA}$  ( $\Delta d = 16.5\text{ \AA}$ ) on cholesterol solubilization, and for the

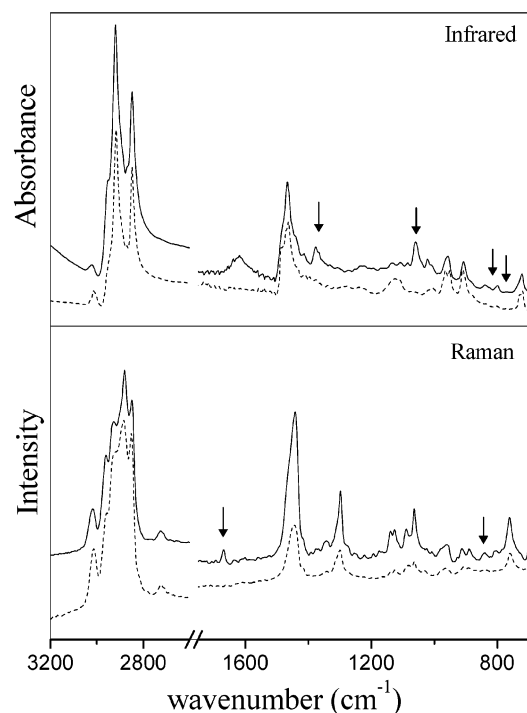


**Figure 4.** Infrared and Raman spectra of the cholesterol-bound intercalated surfactant bilayer. The spectrum of the intercalated bilayer in the absence of cholesterol is shown in dashed lines. The cholesterol bands are indicated with arrows.

intercalated ODTA ( $n = 18$ ) bilayer, the spacing increases from 36.5 to 53.5 Å ( $\Delta d = 17.0$  Å).

The increased lattice spacing of the intercalated surfactant bilayers on solubilization of cholesterol may be related to the location and orientation of the solubilized cholesterol molecule and its effect on the “tilt angle” of the methylene chains of the intercalated bilayer. The orientation of the solubilized cholesterol and its effect on the tilt of the methylene chains of the bilayer were determined from the orientation dependence of the infrared spectra of crystals of the cholesterol-solubilized intercalated bilayer. Before discussing the orientation dependence, a brief overview of the vibrational spectrum of the cholesterol-solubilized intercalated surfactant bilayer is presented.

**Vibrational Spectroscopy.** The infrared and Raman spectra of the cholesterol-solubilized intercalated surfactant bilayer in the region of 4000–600  $\text{cm}^{-1}$  is shown in Figure 4 (the spectrum of the intercalated surfactant bilayer is shown in dashed lines). The subsequent results and discussions are restricted to the CTA ( $n = 16$ ) intercalated surfactant bilayer. The infrared spectrum shows bands due to the solubilized cholesterol, as well as the intercalated surfactant cation. Even though there is an overlap of bands arising from the cholesterol side chain and the intercalated cationic surfactant, several characteristic bands of cholesterol may be distinguished from the bands due to the surfactant cation. The observed band positions along with their assignments are given as a table as part of the Supporting Information.

The dominant features of the infrared spectra are the methylene symmetric and antisymmetric stretching modes at 2848 and 2918  $\text{cm}^{-1}$  and the methylene scissoring and rocking modes of the intercalated CTA chain at 1467 and 720  $\text{cm}^{-1}$  respectively. These assignments are similar to those of the intercalated bilayer in the absence of solubilized cholesterol.<sup>3</sup> The frequencies of the methylene stretching modes indicate a high degree of trans conformational order.<sup>3,21,22</sup> Bands due to the solubilized cholesterol appear at 1059  $\text{cm}^{-1}$ , assigned to

the C–O stretching mode, and at 798 and 839  $\text{cm}^{-1}$ , which are assigned to the sterol ring modes.<sup>23</sup> The position of the C–O stretching mode has been used to characterize the extent of H-bonding involving the cholesterol molecule. In  $\text{CCl}_4$  solution, the band appears at 1051  $\text{cm}^{-1}$  and shifts to higher frequencies with increasing H-bonding.<sup>23</sup> The position of the C–O stretching mode in the solubilized cholesterol is identical to that in crystalline cholesterol (see Supporting Information).

The Raman spectrum, too, shows bands characteristic of the solubilized cholesterol, as well as the intercalated surfactant. The bands at 2880 and 2850  $\text{cm}^{-1}$  are assigned to the antisymmetric and symmetric stretching modes of the methylene groups. The band at 3016  $\text{cm}^{-1}$ , as in the case of infrared, is assigned to the asymmetric stretching mode of the  $\text{N}^+(\text{CH}_3)_3$  “head” group. The band at 1446  $\text{cm}^{-1}$  is assigned to the methylene scissoring mode, and the 1297  $\text{cm}^{-1}$  band is assigned to the methylene twisting mode. The bands due to the solubilized cholesterol molecule are seen at 1670  $\text{cm}^{-1}$ , assigned to the C=C stretching mode, and 699  $\text{cm}^{-1}$  due to the sterol ring mode.

**Orientation of the Solubilized Cholesterol and the Intercalated Surfactant Bilayer.** The orientation of the solubilized cholesterol and its effect on the tilt of the methylene chains of the bilayer was determined from the orientation dependence of the infrared spectra of crystals of the cholesterol-solubilized intercalated bilayer. The orientation was determined from the dichroic ratio of the cholesterol and methylene vibrational modes, which are easily distinguished in the infrared spectrum. The dichroic ratio  $I_\phi/I_{\phi+90}$  was determined for different angles,  $\phi$ , between the electric field vector,  $\mathbf{E}$ , of the incident infrared and the interlamellar normal,  $\mathbf{C}^*$ , from the spectra recorded for two orientations,  $\mathbf{E} \perp \mathbf{C}^*$  and  $\mathbf{E} \parallel \mathbf{C}^*$  ( $I_\phi$  is the intensity of the vibrational mode for an angle  $\phi$ ). The ratio peaks at the angle at which the transition dipole moment of the vibrational mode is parallel to the electric field vector of the incident radiation, from which the orientation of the bond (molecule) with respect to the interlayer normal can be obtained.<sup>24,25</sup>

The orientation of the methylene chains of the bilayer was determined from the dichroic ratio of the methylene rocking mode at 720  $\text{cm}^{-1}$  (Figure 5). This mode has its dipole moment normal to the methylene chain axis. For the intercalated bilayer and the bilayer with cholesterol, the ratio peaks at almost identical values, 36° and 40°, respectively. The corresponding tilt angles, the angle that the molecular axis of the trans methylene chain makes with the interlayer normal, are 54° and 50°, respectively. The presence of solubilized cholesterol, therefore, does not result in any significant decrease in the tilt of the methylene chains of the intercalated bilayer.

The orientation of the solubilized cholesterol molecules was determined from the orientation dependence of the C–O stretching mode of cholesterol appearing at 1060  $\text{cm}^{-1}$ . The spectra in the C–O stretching region of the cholesterol-solubilized intercalated surfactant bilayer for the two orientations,  $\mathbf{E} \perp \mathbf{C}^*$  and  $\mathbf{E} \parallel \mathbf{C}^*$ , are shown in Figure 5c. The corresponding dichroic ratio of the cholesterol C–O stretching mode (Figure 5f) peaks at 20°. Because the transition dipole moment of the C–O stretching mode is along the C–O bond, the dichroic ratio indicates that the C–O bond is oriented at an angle of 20° with respect to the interlamellar normal. The cholesterol molecule is rigid but nonplanar. To determine the orientation of the cholesterol molecule, we construct a hypothetical molecular plane by considering the plane containing the axis joining carbon atoms 3 and 16 (Scheme 1). The C–O bond makes an angle of 25° with respect to this axis of the



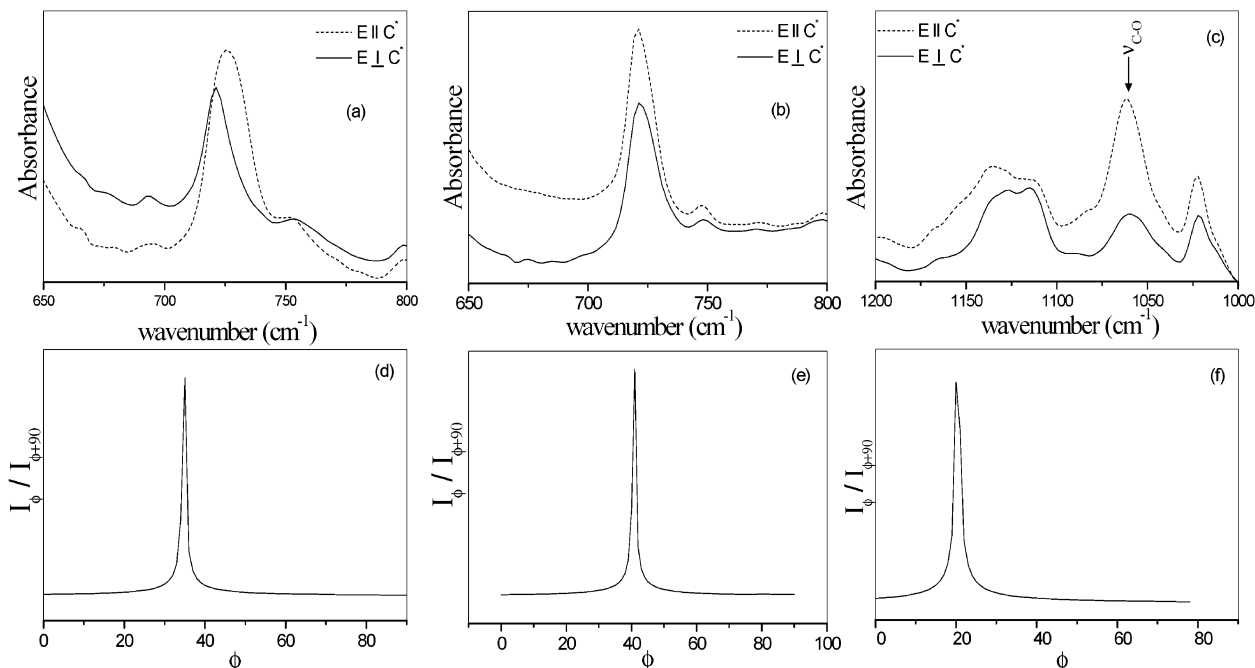
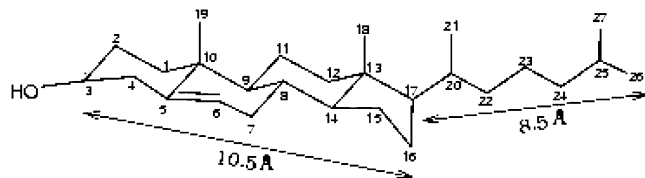


**Figure 5.** Orientation-dependent infrared spectra of the intercalated bilayer in the methylene rocking mode region for two orientations,  $E \perp C^*$  and  $E \parallel C^*$ , (a) in the presence of solubilized cholesterol and (b) in the absence of cholesterol. The corresponding dichroic ratios,  $I_\phi/I_{\phi+90}$ , plotted as a function of  $\phi$  are shown in panels e and d. The orientation-dependent spectra in the cholesterol C–O stretching region of the cholesterol-solubilized intercalated bilayer is shown in panel c, and panel f shows the corresponding dichroic ratio ( $\phi$  is the angle that the electric dipole of the incident IR beam,  $E$ , makes with the interlamellar normal,  $C^*$ ).

#### SCHEME 1



sterol ring of the cholesterol molecule.<sup>26</sup> This, therefore, implies that the molecular plane of the rigid sterol rings are oriented at an angle of 45° (20° + 25°) away from the interlamellar normal, roughly parallel to the molecular axis of the methylene chains (tilt angle 50°) of the intercalated bilayer.

**Effect of Cholesterol Solubilization on Alkyl Chain Conformation of the Intercalated Surfactant Bilayer.** The position of the methylene stretching modes in the infrared spectrum indicates an apparent greater degree of trans ordering of the intercalated surfactant chain on cholesterol solubilization.<sup>21,22</sup> This region, however, has contributions from the cholesterol methylene modes and hence is not a reliable measure of methylene chain conformation. In fact, most spectral regions in the infrared (and for that matter the Raman, too) that are sensitive to the local conformation of the methylene chain have contributions from the alkyl chain part of the cholesterol molecule.

Understanding how cholesterol influences the conformation in alkyl chain assemblies, such as lipid bilayers, by spectroscopic techniques is generally a difficult exercise because it is not possible to separate the contribution of the methylene tail of the cholesterol from that of the alkyl chain of the bilayer, except by isotope labeling. We have circumvented this problem by analyzing those features of the vibrational spectra that are characteristic of the global conformation of the methylene chain and are therefore dependent on the chain length. These are the progression bands in the infrared, which arise from the coupling of the vibrational modes of methylene units that are in trans

registry.<sup>27–31</sup> These bands correspond to modes delocalized over the length of the chain of which the spacing and frequency depend on the number of coupled trans methylene units. Appropriate for the present study are the progression bands arising from the coupling of wagging modes of trans methylene units because they appear in a spectral region of the infrared that is free of cholesterol bands. We had shown previously, from an analysis of the progression band intensities and spacing, that in the pure intercalated bilayer a majority of the methylene chains adopt a planar all-trans conformation at low temperatures (50 K) with the concentration of planar chains, as expected, decreasing with temperature.<sup>3,19</sup> This was determined by monitoring the intensity of the progression bands as function of temperature; the presence of a single gauche defect in a chain decouples the vibrational modes and such chains no longer contribute to the intensity. The intensity of the progression bands is, therefore, directly proportional to the concentration of all-trans planar chains present in the intercalated bilayer.

The methylene wagging progression bands of the intercalated surfactant (CTA) bilayer with and without solubilized cholesterol at different temperature is shown in Figure 6 (the spectra have been normalized<sup>32</sup> using the C–N<sup>+</sup> stretching band at 910 cm<sup>−1</sup>). The frequencies of the wagging progression bands are identical for the intercalated surfactant bilayer with and without solubilized cholesterol and, as shown previously, are characteristic of all 15 methylene units of the CTA chain in trans conformational registry.<sup>31</sup> For both compounds, there is no change in the positions or spacing of the progression bands with temperature (Figure 6), the only change being in the intensities of these bands. The methylene progression band intensities are comparable at low temperature (75 K), but at room temperature (310 K), the progression band intensities are much higher for the cholesterol-solubilized bilayer indicating a higher concentration of planar all-trans methylene chains.

The intensities of the progression bands have been used by Mendelsohn et al.<sup>30,33,34</sup> in their study of alkyl chain conforma-

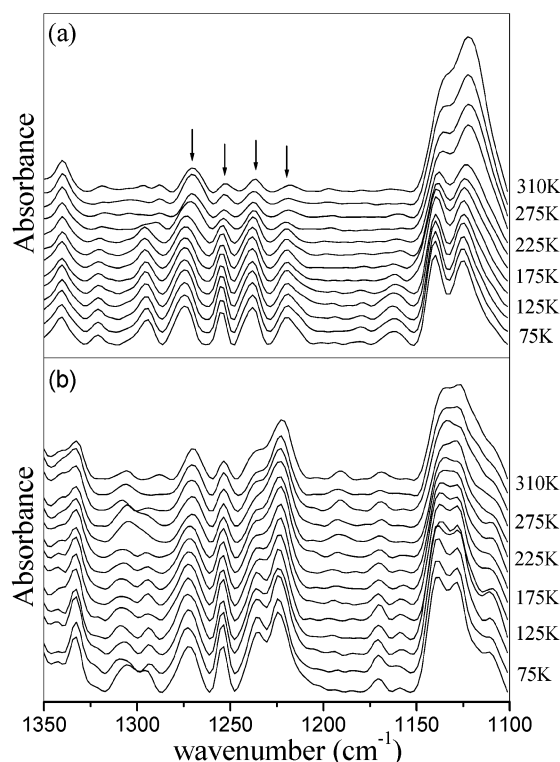


**Figure 6.** Infrared spectra in the methylene wagging progression region for (a) the intercalated surfactant bilayer and (b) the cholesterol-bound intercalated surfactant bilayer recorded at different temperatures (the wagging progression bands are indicated with arrows).

tion in bilayer dispersions of 1,2-dipalmitoyl phosphatidylcholine (DPPC), as well as DPPC–cholesterol mixtures, across the phase transitions. The intensity of the methylene wagging band progression bands at different temperatures for the DPPC–cholesterol bilayer dispersions were compared with the intensity of these bands in pure DPPC dispersions. The results indicated that the incorporation of cholesterol into the DPPC bilayer dispersion resulted in the persistence of trans conformational order even at temperatures well above the phase-transition temperature of the DPPC bilayer, whereas for the pure DPPC bilayer phase, it was found to vanish rapidly near the phase transition.<sup>30,33,34</sup>

A comparison of the temperature variation of the intensities of the progression bands of the cholesterol-solubilized intercalated bilayer and the intercalated bilayer is shown in Figure 7. The intensity,  $I_T$ , at temperature  $T$  has been normalized with respect to the intensity at 60 K ( $I_{60K}$ ),  $I_T/I_{60K}$ , for both compounds enabling direct comparison between the two samples. The intensities do not change below 75 K for both of the phases, and hence, it is reasonable to assume that all intercalated methylene chains, in both compounds, adopt an all-trans conformation at this temperature. The normalized intensity at any temperature is, therefore, a direct measure of the fraction of all-trans intercalated methylene chains present at that temperature. The temperature variation of the normalized intensities directly characterizes the temperature evolution of all-trans conformational order in the bilayer. The normalized intensity of the progression bands for the pure bilayer phase, as well as the cholesterol-solubilized bilayer phase, follow an almost similar trend up to 200 K. Above this temperature, however, the intensity of the progression bands drops more rapidly in the absence of cholesterol, the normalized intensity dropping to a value of 0.24 by 300 K. For the cholesterol-bound surfactant bilayer, however, the intensity appears to plateau at a value of

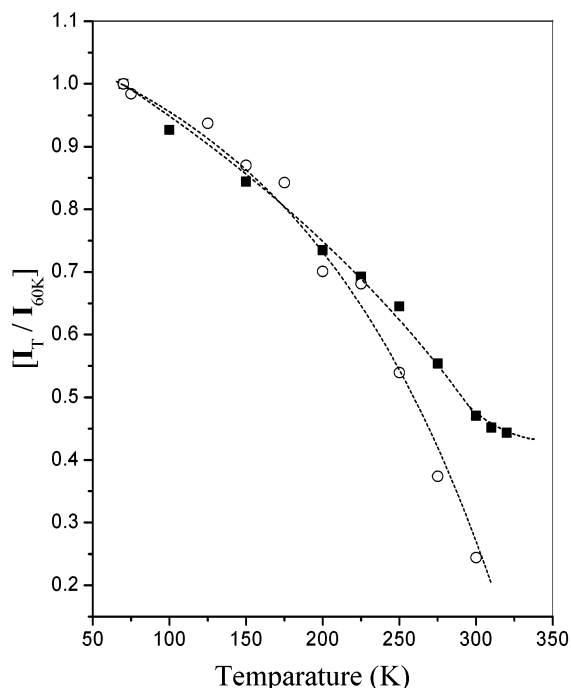


**Figure 7.** Thermal variation of the fraction of all-trans methylene chains in the bilayer with and without solubilized cholesterol. The plots show the temperature dependence of the normalized intensity of the progression bands of the intercalated bilayer (○) and cholesterol-solubilized bilayer (■). The dashed line is a guide to the eye.

~0.45. As mentioned earlier, the normalized intensities are indicative of the fraction of planar (all-trans) methylene chains. Figure 7 shows that the effect of cholesterol is that for ~50% of the intercalated CTA ions the all-trans conformation persists even at temperatures at which in the absence of cholesterol the concentration of planar conformations are negligible. The fact that below 200 K the temperature variation of the concentration of planar conformers is similar suggests that even when cholesterol is present in the bilayer, some of the surfactant chains behave as those in the pure bilayer. The remaining chains, in contrast, adopt an all-trans planar conformation at all temperatures.

It is clear that cholesterol inhibits the rotameric freedom of the methylene chains in the intercalated bilayer forcing them into an all-trans conformation. These are likely to be chains in the immediate neighborhood of a cholesterol molecule because an all-trans methylene chain conformation would favor hydrophobic interactions with the rigid steroid ring of the cholesterol. Molecular simulation of lipid–cholesterol interactions, too, had arrived at a similar conclusion.<sup>35</sup> Such a model could also explain the significance of only half the chains in the bilayer being affected in the presence of cholesterol. Because the cholesterol to intercalated CTA ratio is ~0.25 and assuming that two methylene chains “sandwich” a cholesterol molecule, then only half of the intercalated surfactant molecules of the bilayer directly neighbor a cholesterol molecule. The remaining half is unaffected, and the thermal evolution of conformational disorder of these chains is identical to that of methylene chains in the pure intercalated bilayer. It thus appears that surfactant chains in the intercalated bilayer once-removed from a cholesterol molecule behave as if cholesterol is not present.

**The Binding of Cholesterol to the Intercalated Surfactant Bilayer.** From the experimental results of X-ray diffraction and vibrational spectroscopy, it is possible to construct a model of the binding of cholesterol with the methylene chains of the intercalated bilayer. Cholesterol may be solubilized in the

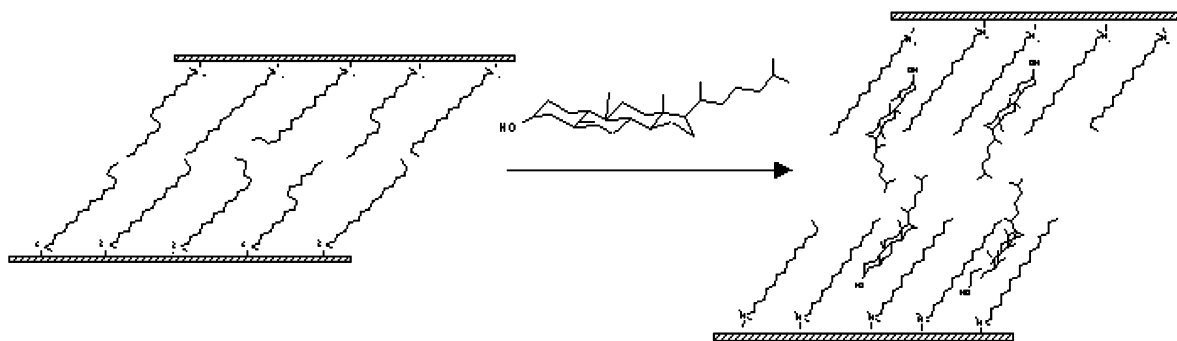


**Figure 8.** Schematic representation of the binding of cholesterol to the intercalated bilayer. The increase in lattice spacing on solubilization of cholesterol is  $\sim 17.0$  Å.

intercalated surfactant bilayer,  $\text{Cd}_{0.83}\text{PS}_3(\text{C}_n\text{TA})_{0.34}$ ; the molar ratio of the cholesterol to intercalated surfactant has a unique value of 0.25:1, irrespective of the method of preparation. The intercalated  $\text{C}_n\text{TA}$  ( $n = 16, 18$ ) surfactant chains are devoid of any functional group, and consequently, hydrogen bonding between the cholesterol and the intercalated surfactant chains can be ruled out. The interactions are, therefore, purely dispersive or hydrophobic in character. The lattice expansion upon cholesterol solubilization is  $\sim 17$  Å for both the  $n = 16$  and  $n = 18$   $\text{C}_n\text{TA}$  intercalated chains. This expansion cannot be accounted for by the observed decrease in tilt angles of the all-trans methylene chains of the bilayer in the presence of cholesterol. The change in tilt angle can, at best, account for an expansion on solubilization of  $\sim 3$  Å. A comparison of the molecular dimensions of the cholesterol molecule (see Scheme 1) indicates that the increase in lattice spacing is approximately twice the length ( $\sim 8.5$  Å) of the hydrocarbon “tail” of the cholesterol. This suggests that the “tail” is not embedded in the bilayer and only the steroid moiety is located in the bilayer. A cartoon of the proposed structure of cholesterol bound to the intercalated surfactant bilayer is shown in Figure 8. In this model, the steroid moieties are located within the intercalated bilayer but the hydrocarbon “tail” of the cholesterol, probably because it is small and does not pack as well, dangles in the gap created on solubilization of cholesterol. The conformation of cholesterol “tail” shown in Figure 8 is known to exist in the crystalline state of cholesterol.<sup>26</sup> It may be recalled that the mean head-to-head separation in the intercalated surfactant bilayer<sup>3</sup> is 9 Å; sufficient space is therefore available to accommodate the sterol moiety in the bilayer.

The arrangement shown in Figure 8 in which two all-trans methylene chains sandwich a rigid cholesterol molecule would optimize dispersive interactions between the hydrocarbon chain of the intercalated surfactant bilayer and the almost planar steroid molecule while still allowing for a great degree of conformational freedom for the hydrocarbon “tail” of the cholesterol molecule. A perspective view of this arrangement is shown in Figure 9. The sterol part of the cholesterol molecule is almost planar and relatively rigid, and consequently, conformational freedom of intercalated surfactant methylene chains encountering the steroid molecule would be hindered and forced to adopt all-trans planar structure. The tilt angle of the methylene chains ( $\sim 50^\circ$ ) and of the sterol ring of the cholesterol molecules ( $\sim 45^\circ$ ) indicates that they are approximately parallel. An exact parallel configuration is probably not possible because the cholesterol molecule is flat only on one side while from the other side methyl groups project. Vibrational spectroscopy provides support for such a model. The spectra show that half of the intercalated surfactant chains of the bilayer with a cholesterol/intercalated CTA molar ratio of 0.25 are planar at

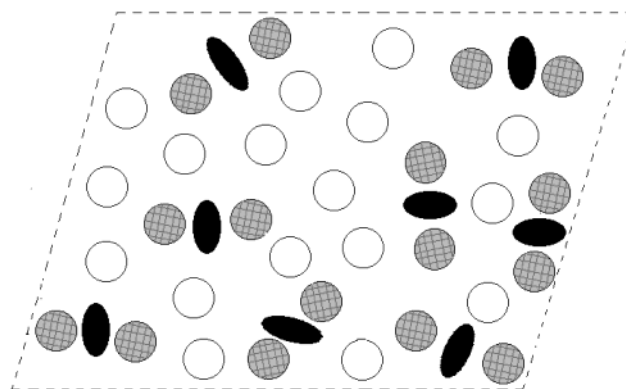


**Figure 9.** Perspective view, looking down the interlayer normal (the  $C^*$  axis), of the cholesterol-bound intercalated surfactant bilayer. The ratio of cholesterol molecules, represented by ellipsoids, to surfactant chains, shown as circles, is 1:4. Surfactant chains neighboring a cholesterol molecule, shown by filled circles, adopt an all-trans conformation at all temperatures; the remaining chains enjoy a greater degree of conformational freedom.

room temperature, whereas in the absence of cholesterol, less than 20% of the intercalated chains are planar. The vibrational spectra also indicate that the influence of the solubilized cholesterol is short-ranged. The conformation and thermal behavior of surfactant chains once-removed are unaffected by the presence of cholesterol and behave as those in the pure intercalated surfactant bilayer. This is understandable because no great advantage in terms of dispersive interactions is obtained by surfactant chains not in contact with the cholesterol molecule adopting a rigid planar structure. Our experiments show that in the presence of cholesterol two types of alkyl chains may be distinguished in the bilayer—one of which the rotameric conformational freedom is unaffected and the other of which the freedom is inhibited and which is forced to adopt a rigid, planar, all-trans conformation at all temperatures.

**Supporting Information Available:** Observed band positions and assignments in the infrared spectrum of cholesterol and cholesterol-bound intercalated surfactant bilayer. This material is available free of charge via the Internet at <http://pubs.acs.org>.

## References and Notes

- (1) Lagaly, G. *Angew. Chem., Int. Ed. Engl.* **1975**, *15*, 575.
- (2) Ogawa, M.; Kuroda, K. *Bull. Chem. Soc. Jpn.* **1997**, *70*, 2593.
- (3) Venkataraman, N. V.; Vasudevan, S. *J. Phys. Chem. B* **2001**, *105*, 1805.
- (4) Yeagle, P. L. *Biochim. Biophys. Acta* **2001**, *822*, 267.
- (5) Vist, M. R.; Davis, J. H. *Biochemistry* **1990**, *29*, 451.

- (6) Presti, F. T. In *Membrane Fluidity in Biology: Cellular Aspects*; Alola, R. C., Boggs, J. M., Eds.; Academic Press: New York, 1985; pp 97–146.
- (7) Mabrey, S.; Sturtevant, J. M. *Proc. Natl. Acad. Sci. U.S.A.* **1976**, *73*, 3862.
- (8) Demel, R. A.; Bruckdorfer, K. R.; vanDeenen, L. L. M.; *Biochim. Biophys. Acta.* **1972**, *255*, 311.
- (9) Jacobs, R.; Oldfield, E. *Biochemistry* **1979**, *18*, 3280.
- (10) Delmelle, M.; Butler, K. W.; Smith, I. C. P. *Biochemistry* **1980**, *19*, 698.
- (11) McMullen, T. P. W.; McElhanney, R. N. *Curr. Opin. Colloid Interface Sci.* **1996**, *1*, 83.
- (12) Bhattacharya, S.; Haldar, S. *Biochim. Biophys. Acta.* **2000**, *1467*, 39.
- (13) Karolis, C.; Coster, H. G. L.; Chilcott, T. C.; Barrow, K. D. *Biochim. Biophys. Acta.* **1998**, *1368*, 247.
- (14) Ouvrard, G.; Brec, R.; Rouxel, J. *Mater. Res. Bull.* **1985**, *20*, 1181.
- (15) Brec, R. *Solid State Ionics* **1986**, *22*, 3.
- (16) Clement, R. R. *J. Chem. Soc., Chem. Commun.* **1980**, 647.
- (17) (a) Clement, R.; Garnier, O.; Jegoudez, J. *Inorg. Chem.* **1986**, *25*, 1404. (b) Clement, R.; Audiere, J. P.; Renard, J. P. *Rev. Chim. Miner.* **1982**, *19*, 560.
- (18) Jeevanandam, P.; Vasudevan, S. *Solid State Ionics* **1997**, *104*, 45.
- (19) Venkataraman, N. V.; Vasudevan, S. *Proc.—Indian Acad. Sci. Chem. Sci.* **2001**, *113*, 539.
- (20) Venkataraman, N. V.; Mohanambe, L.; Vasudevan, S. *J. Mater. Chem.* **2003**, *17*, 170.
- (21) MacPhail, R. A.; Strauss, H. L.; Snyder, R. G.; Elliger, C. A. *J. Phys. Chem* **1984**, *88*, 334.
- (22) Snyder, R. G.; Strauss, H. L.; Elliger, C. A. *J. Phys. Chem.* **1982**, *86*, 5145.
- (23) Umemura, J.; Cameroon, D. G.; Mantsch, H. H. *Biochim. Biophys. Acta.* **1980**, *602*, 32.
- (24) Arun, N.; Vasudevan, S.; Ramanathan, K. V. *J. Am. Chem. Soc.* **2000**, *122*, 6028.
- (25) Venkataraman, N. V.; Vasudevan, S. *J. Phys. Chem. B* **2000**, *104*, 11179.
- (26) Shieh, S.; Hoard, L. G.; Norman, C. E. *Acta Crystallogr.* **1981**, *B37*, 1538.
- (27) Snyder, R. G. *J. Mol. Spectrosc.* **1960**, *4*, 411.
- (28) Snyder, R. G.; Schachtschneider, J. H. *Spectrochim. Acta.* **1963**, *19*, 85.
- (29) Tasumi, M.; Shimonauchi, T.; Miyazawa, T. *J. Mol. Spectrosc.* **1962**, *9*, 261.
- (30) Chia, N. C.; Vilchère, C.; Bittman, R.; Mendelsohn, R. *J. Am. Chem. Soc.* **1993**, *115*, 12050.
- (31) (a) Venkataraman, N. V.; Vasudevan, S. *J. Phys. Chem. B* **2001**, *105*, 7639. (b) **2002**, *106*, 7766.
- (32) Snyder, R. G.; Cameroon, D. G.; Casal, H. L.; Compton, D. A. C.; Mantsch, H. H. *Biochim. Biophys. Acta.* **1982**, *684*, 111.
- (33) Chia, N. C.; Mendelsohn, R. *J. Phys. Chem.* **1992**, *96*, 10543.
- (34) Senak, L.; Moore, D.; Mendelsohn, R. *J. Phys. Chem.* **1992**, *96*, 2749.
- (35) Scott, H. L. *Biophys. J.* **1991**, *59*, 445.